Robles Martínez, Á.; Ruano García, MV.; Ribes Bertomeu, J.; Seco Torrecillas, A.; Ferrer, J. (2014). Global sensitivity analysis of a filtration model for submerged anaerobic membrane bioreactors (AnMBR). Bioresource Technology. 158:365-376. doi:10.1016/j.biortech.2014.02.087.

Global sensitivity analysis of a filtration model for submerged anaerobic membrane bioreactors (AnMBR)

A. Robles[a,*], M.V. Ruano[a,1], J. Ribes[a], A. Seco[a] and J. Ferrer[b]

[a] Departament d'Enginyeria Química, Escola Tècnica Superior d'Enginyeria, Universitat de València, Avinguda de la Universitat s/n, 46100 Burjassot, Valencia, Spain (e-mail: *angel.robles@uv.es; mavictoria.ruano.garcia@fcc.es; josep.ribes@uv.es; aurora.seco@uv.es)*

[b] Institut Universitari d'Investigació d'Enginyeria de l'Aigua i Medi Ambient, IIAMA, Universitat Politècnica de València, Camí de Vera s/n, 46022 Valencia, Spain (e-mail: *jferrer@hma.upv.es*)

* Corresponding author: tel. +34 96 387 99 61, fax +34 96 387 90 09, e-mail: *angel.robles@uv.es*

Abstract

The results of a sensitivity analysis of a filtration model for submerged anaerobic MBRs (AnMBRs) are assessed in this paper. This study aimed to (1) identify the less-(or non-) influential factors of the model in order to facilitate model calibration and (2) validate the modelling approach (i.e. to determine the need for each of the proposed factors to be included in the model). The sensitivity analysis was conducted using a revised version of the Morris screening method. The dynamic simulations were conducted using long-term data obtained from an AnMBR plant fitted with industrial-scale hollow-fibre membranes. Of the 14 factors in the model, six were identified as influential, i.e. those calibrated using off-line protocols. A dynamic calibration (based on optimisation algorithms) of these influential factors was conducted. The resulting estimated model factors accurately predicted membrane performance.

[1] **Present address:** aqualia, gestión integral del agua, S.A. Avenida del Camino de Santiago, 40 28050 Madrid, Spain

Keywords

Filtration model; global sensitivity analysis; industrial-scale hollow-fibre membranes; Morris screening method; submerged anaerobic membrane bioreactor (AnMBR)

Highlights

A global sensitivity analysis of a filtration model for AnMBRs was conducted.

It was conducted using a revised version of the Morris screening method.

Sensitivity results significantly simplified the input subset to be calibrated.

Only one input factor could be removed from the model.

1. Introduction

Understanding and optimising a complex system such as a membrane bioreactor (MBR) is a difficult and time-consuming process mainly because of the large number of sub-processes taking place simultaneously, which are generally highly dependent upon each other. In this respect, mathematical modelling is a powerful tool for studying such complex systems (Naessens et al., 2012).

Certain models have been found to be useful for dealing with different aspects of WWTPs, e.g. R&D of wastewater treatment processes, design and upgrading of WWTPs, and the development of operating and control strategies designed to optimise process performance (Ferrer et al., 2004; Derbal et al., 2009; Ruano et al., 2012b). Computerised models make it possible to perform many virtual experiments in a short space of time. Therefore the mathematical modelling of filtration in submerged anaerobic MBRs (AnMBRs) may help gain an insight into the key factors in membrane fouling (Mannina et al., 2011), and are also invaluable for the design, prediction and

control of the membrane technology used for treating wastewater (Ng and Kim, 2007). However, predictions made on the basis of models are not free from uncertainty because models are an abstract approximation of reality and are usually based on a considerable number of assumptions. In this respect, sensitivity analysis provides useful information for modellers because it attempts to quantify how changes to a model's input factors affect the model's output. In addition, due to the limited data available about full-scale systems, the subset of identifiable factors can be reduced, which makes calibrating the model simpler.

The different sensitivity analysis strategies applied in literature are usually classified in two main categories: global sensitivity analysis (GSA) which involves sampling and whose range of input uncertainty reflects the uncertainty in the output variables; and local sensitivity analysis, which is based on the local impact of input factors upon output variables.

The Morris screening method (Morris, 1991) is a one-at-a-time (OAT) method of GSA which calculates the elementary effects (EE_i) of input factors upon the output of a model. This screening method makes it possible to validate the modelling approach because it identifies the non-influential input factors, which could be useful for improving the definition of the model by evaluating the usefulness of the non-influential input factors.

One key issue with the Morris screening method is that the sampling matrix is generated at random. This random sampling may not represent the sampling space well and result in an inadequate screening of non-influential input factors. In this regard, Campolongo et al. (2007) proposed an improved sampling method which maximised the

distances between the final trajectories (*r*) selected. However, this improved sampling was not suitable for large models because of the vast numbers of calculations needed to determine the best combinations. For this reason, Ruano et al. (2012a) proposed an improved sampling method based on trajectory design intended to overcome the great many calculations required by the Campolongo sampling method.

In this study, a revised version of the Morris screening method that includes an improved sampling method (Ruano et al., 2012a) was applied to a filtration model (resistance-in-series-based) for submerged AnMBRs (Robles et al., 2013a; 2013b). Although the model was proven to be robust, the Morris screening method was used not only to identify the less/non-influential input factors of the model, but also to validate the modelling approach (i.e. to assess the need to include each of the proposed factors in the model). In addition, a dynamic calibration (based on optimisation algorithms) of the most influential input factors was conducted.

2. Materials and methods

2.1. AnMBR plant description

The filtration model evaluated in this study was developed, calibrated and validated using data obtained from a AnMBR system fitted with industrial-scale submerged hollow-fibre (HF) membranes and fed with urban wastewater from the pre-treatment of the Carraixet WWTP (Valencia, Spain). The plant consists of an anaerobic reactor with a total volume of 1.3 m^3 (0.4 m^3 head space for biogas) connected to two membrane tanks each with a total volume of 0.8 m^3 (0.2 m^3 head space for biogas). Each membrane tank (MT) has one industrial HF ultrafiltration membrane unit (PURON®,

Koch Membrane Systems (PUR-PSH31) with 0.05 µm pores). Each module has a total membrane surface of 30 m^2. For further details of this AnMBR system, see Robles et al. (2013c).

2.2. Monitoring system

In addition to being monitored on line, grab samples of anaerobic sludge were taken once a day to assess filtration performance. MLTS concentration was determined according to Standard Methods (2005) using procedure 2540 B.

2.3. Model description

The filtration model used in this study (Robles et al., 2013a; 2013b) gives the dynamic evolution of the transmembrane pressure (TMP) by applying Eq. 1 and Eq. 2.

$$TMP(t) = J \cdot \mu \cdot R_T \qquad \text{(Eq. 1)}$$

where:

- J is the transmembrane flux (m s^{-1})
- μ is the permeate dynamic viscosity (kg m^{-1} s)
- $TMP\ (t)$ is the transmembrane pressure (Pa)
- R_T is the total filtration resistance (m^{-1})

$$R_T = R_M + R_C + R_I = R_M + \omega_C \cdot \alpha_C + \omega_I \cdot \alpha_I \qquad \text{(Eq. 2)}$$

where:

- R_M is the intrinsic membrane resistance (m^{-1})

- R_C is the cake layer resistance (m^{-1})
- R_I is the irreversible fouling resistance (m^{-1})
- ω_C is the mass of cake deposited per membrane area (kg m^{-2})
- α_C is the average specific cake resistance (m kg^{-1})
- ω_I is the mass of irreversible fouling per membrane area (kg m^{-2})
- α_I is the average specific irreversible fouling resistance (m kg^{-1})

To account for cake layer compression, α_C was defined as time- and TMP-dependent as per Bugge et al. (2012) and Jørgensen et al. (2012). In addition, to account for sub-critical fouling, an additional dependence of α_C on time was considered in the model (Robles et al., 2013a), as shown in Eq. 3 below:

$$\alpha_C(t) = \alpha_C(t-\Delta t) + \max\left(k_{SF}, k_t \cdot \left(\alpha_{C,0} \cdot \left(1 + \frac{TMP}{TMP_a}\right) - \alpha_C(t-\Delta t)\right)\right) \cdot \Delta t \qquad \text{(Eq. 3)}$$

Where:

- $\alpha_C(t)$ is the specific resistance of the cake at time t (kg m^{-2}).
- $\alpha_C(t-\Delta t)$ is the specific resistance of the cake at a previous moment in time (kg m^{-2}).
- k_{SF} is the parameter related to sub-critical fouling (kg m^{-2} s^{-1}).
- $\alpha_{C,0}$ is the specific resistance of the cake at zero pressure (kg m^{-2})
- TMP_a is the pressure needed to double the specific resistance (Pa)
- k_t is the time constant (s^{-1}).
- Δt is the time step (s).

To model the dynamics of ω_C and ω_I a black-box approach was adopted in the model. This approach considers 3 suspended components: MLTS concentration X_{TS} (kg TS m^{-3}); dry mass of cake on the membrane surface, X_{m_C} (kg TS); and dry mass of irreversible fouling on the surface of the membrane, X_{m_I} (kg TS). In addition, this approach includes four kinetically governed physical processes: (1) cake layer build-up during filtration; (2) cake layer removal using biogas sparging to scour the membrane; (3) cake layer removal during back-flushing; and (4) consolidation of irreversible fouling. Table 1 shows the stoichiometry and kinetic formulae of the four processes considered in the model.

Process 1 (cake layer build-up) is the convective transport of foulants (X_{TS} in the model) to the membrane, which is a function of the permeate flow-rate, Q_{20P} (m^3 s^{-1}), and bulk concentration (X_{TS}). Process 2 (membrane scouring by biogas sparging) is the impact of the hydrodynamic conditions in the membrane tank caused by biogas sparging (measured as BRF_V: biogas recycling flow per bulk volume in the membrane tank). A maximum membrane scouring velocity ($q_{MS,Max}$) was defined for process 2. In process 3, the back-flushing removal rate is defined as a function of the back-flushing flow rate, Q_{20BF} (m^3 s^{-1}), and X_{m_C}. As per Sarioglu et al. (2012), a maximum back-flushing removal velocity was defined, $q_{BF,Max}$ (m^{-3}), for process 3.

One half-saturation switching function ($M_{X_{m_C}}$, Eq. 4) for both membrane scouring (process 2) and back-flushing (process 3) was used to vary the removal of solids smoothly as the cake layer disappeared (Sarioglu et al., 2012).

$$M_{X_{m_C}} = \frac{X_{m_C}}{K_{S,X_{m_C}} + X_{m_C}} \qquad \text{(Eq. 4)}$$

where:

- $K_{S,X_{mC}}$ is the half-saturation coefficient of cake solids during membrane scouring and back-flushing (kg ST).

Process 2 includes one sigmoid inhibition function (I_{MS}, Eq. 5) to model the impact of filtering above or below critical conditions.

$$I_{MS} = \frac{1}{1 + K_F \cdot e^{\left(J_{20} \cdot \left(\beta_1 \cdot BRF_V + \beta_2 \cdot MLTS + \gamma\right)\right)}} \quad \text{(Eq. 5)}$$

where:

- K_F is the adjustment parameter representing the fouling rate when the gross 20 ºC-normalised transmembrane flux (J_{20}) tends to zero (Pa s^{-1}).
- J_{20} is the gross 20 ºC-normalised transmembrane flux (m s^{-1}).
- BRF_V is the biogas recycling flow per bulk volume in the membrane tank (Nm^3 s^{-1} m^{-3}).
- $MLTS$ is the mixed liquor total solids concentration (kg m^{-3}).
- β_1 (s^2 m^{-1}), β_2 (s m^2 kg^{-1}) and γ (s m^{-1}) are the parameters of the model.

On the basis of long-term experimental results, the value of γ was defined as a function of R_I to account for the reduction over time in the filtering capacity of the membranes due to the onset of irreversible fouling. This dependence on irreversible fouling can be expressed as:

$$\gamma_t = \gamma_0 - \left(R_{I_t} - R_{I_0}\right) k_{RI} \quad \text{(Eq. 6)}$$

where:

- γ_t is the value of γ at time t (s m^{-1}).
- γ_0 is the value of γ at the initial time (s m^{-1}).
- R_{I_t} is the irreversible fouling resistance at time t (m^{-1}).
- R_{I_0} is the irreversible fouling resistance at the initial time (m^{-1}).
- k_{RI} is the proportional constant (s).

Finally, irreversible fouling (process 4) was given in the evaluated model as a direct function of X_{m_C} and a maximum irreversible fouling kinetic constant, $q_{IF,Max}$ (s^{-1}).

This filtration model features a total of 14 factors that must be calibrated for each specific system (see Table 2). These factors were previously calibrated by off-line and dynamic calibration methods using short-term and long-term data from the AnMBR plant (Robles et al., 2013a; 2013b). In addition, on the basis of expert knowledge, default values were assigned to those factors that could not be estimated from the available data (Robles et al., 2013a). Table 2 shows these default values calibrated beforehand and used in the sensitivity analysis carried out in this study.

2.4. Simulation

This study included 1 month of dynamic simulations using data obtained from the above-mentioned AnMBR system. This period was selected as a compromise between obtaining reliable results and the cost of calculations. It is important to note that the simulation period must be sufficiently long to enable the effect of both reversible and irreversible fouling mechanisms to be evaluated (Drews, 2010).

Simulation entailed the following dynamic operating conditions recorded during the long-term performance of the AnMBR plant: MLTS levels from approx. 15 – 18 g L^{-1}; biogas recycling flow (BRF) from 4 to 12 Nm^3 h^{-1}; and J_{20} from approx. 4 to 12 LMH. The dynamics in J_{20} considered the fluctuations in the influent flows of WWTPs. For this purpose, the standard dry-weather influent records (updated in 2006) recommended by Copp (1999) were used as shown in Robles et al. (2013d).

2.5. Morris screening method

The Morris screening method (Morris, 1991) is a one-factor-at-a-time method of GSA that evaluates the distribution (F_i) of the elementary effects (EE_i) of each input factor upon model outputs, used to calculate the statistical parameters that provide sensitivity data. In this study the scaled elementary effect (SEE_i) proposed by Sin and Gernaey (2009) was applied. EE_i is in itself a local measure of sensitivity, but this drawback is overcome by repeating *EEi* calculations in the input region of interest using Morris's efficient random sampling strategy, which is obtained by using a trajectory-based design. This sampling strategy then evaluates the *EEi* of each input factor with the same step size but at different initial points in the input region of interest. Finally, the analysis of *Fi* of the elementary effects of each input factor will determine the relative importance of the input factors, providing a good approximation of a GSA.

The finite distribution of elementary effects associated with each input factor F_i is commonly obtained by sampling different coordinates (X) from the input space at random. However, this random sampling of X may only cover a small part of the space. Therefore, in this study the trajectory-based sampling strategy proposed in Ruano et al.

(2012a) was applied. This strategy is based on the improved sampling proposed by Campolongo et al. (2007), which consists in selecting the r trajectories in such a way as to maximise their dispersion in the input space. At first, a high number of random Morris trajectories *M* are generated and then the highest spread r trajectories are chosen out of *M*. This spread is calculated following the definition of distance between a couple of trajectories *m* and *l* defined by Eq. 7.

$$d_{ml} = \left\{ \sum_{i=1}^{k+1} \sum_{j=1}^{k+1} \sqrt{\sum_{z=1}^{k} \left[X_i^m(z) - X_j^l(z) \right]^2} \right. \text{ for } m \neq l \text{ otherwise } d_{ml} = 0 \qquad \text{(Eq. 7)}$$

where:

- $X_i^m(z)$ indicates the *z*th coordinate of the *i*th point of the *m*th Morris trajectory.

Consequently, the best *r* trajectories out of *M* are selected by maximising the distance d_{ml} among them, and thus, the quantity *D*, which is the sum of all the distances d_{ml} between couple of trajectories belonging to the combination. This *D* quantity must be calculated for each possible combination of *r* trajectories. Consequently, the evaluation of all the possible combinations results in a high computational demand. To solve this problem Ruano et al. (2012a) developed an alternative methodology which does not take into account all the possible combinations, but it gets a combination of *r* trajectories out of *M* that are really close to the highest spread one and with low computational demand. Although the proposed sampling does not guarantee maximum overall distances between the final trajectories (*r*) selected (i.e. maximum dispersion in the input space), at least these distances are maximised locally. For further details on this trajectory-based sampling strategy and its comparison with to the Morris' random strategy see Ruano et al. (2012a).

As per Saltelli et al. (2004), the mean (μ), standard deviation (σ) and absolute mean (μ^*) of the SEE_i values of each F_i were used in this study as sensitivity measures. In accordance with Campolongo et al. (2007), it is required to evaluate μ and σ simultaneously to reliably assess stability rankings since an input factor with elementary effects of different sign would have a low value of μ but a considerable value of σ (i.e. identifiable input factors affecting the output non-linearly or interactively). To overcome this problem, as suggested in Campolongo et al. (2007), μ^* was used in this study to rank the input factors in order to systematically identify the optimal number of repetitions of elementary effects calculations (i.e. r_{opt}). μ^* can be also used to systematically differentiate between non-influential input factors (low μ^*) and influential input factors (high μ^*). r_{opt} for each F_i was sought with a constant resolution of $p = 4$. In order to identify r_{opt}, r was sequentially increased until the ranking of input factors remained nearby stable, i.e. type II error was minimised (type II error: identifying an important factor as insignificant). This stability was numerically evaluated using a modified version of the position index $PF_{ri \rightarrow rj}$ proposed by Ruano et al. (2012a). For given rankings obtained by r_i and r_j, this modified index $PF_{ri \rightarrow rj}$ is defined by Eq. 8

$$PF_{r_i \rightarrow r_j} = \sum_{k=1}^{k} \frac{Abs\left(P_{k,i} - P_{k,j}\right)}{\mu_{P_{k,i},P_{k,j}}} \cdot \frac{1}{PF_{MAX}} \qquad \text{(Eq. 8)}$$

where:

- $P_{k,i}$ is the position of the k^{th} input factor in the ranking obtained by r_i
- $P_{k,j}$ is the position of the k^{th} input factor in the ranking obtained by r_j

- $\mu_{P_{k,i},P_{k,j}}$ is the average of the positions of the k^{th} input factor in the ranking obtained by r_i and r_j.
- PF_{MAX} is the maximum value of $PF_{ri \rightarrow rj}$ for the number of input factors evaluated

$PF_{ri \rightarrow rj}$ is maximum when the maximum spread of all factors is obtained for the two rankings compared. For instance, for 3 input factors and $P_{1,i} = 1$, $P_{2,i} = 2$, $P_{3,i} = 3$ the maximum value of $PF_{ri \rightarrow rj}$ occurs when $P_{1,i} = 3$, $P_{2,i} = 1$, $P_{3,i} = 2$ (Cosenza et al., 2013). For 14 input factors PF_{MAX} results in 14.13.On the basis of this position index $PF_{ri \rightarrow rj}$ (Eq. 8) a general criteria for quantifying the convergence of the Morris screening method is established. Based on previous studies, reaching two consecutive $PF_{ri \rightarrow rj}$ values below 0.3 is proposed as criteria for selecting r_j as r_{opt}.

Once r_{opt} was found, the graphical Morris approach was used to identify the factors that influence the model. The μ and σ obtained for all SEE_i values of each F_i are plotted. Two lines were also plotted, corresponding to $\mu_i \pm 2SEM_i$, where SEM_i is the standard error of the mean that can be calculated thus: $SEM_i = \sigma_i / \sqrt{r}$. Factors laying outside the wedge formed by the two lines corresponding to $\mu i = \pm 2SEMi$ (presenting high μ and relatively small σ) are deemed in this study to be influential presenting linear and additive effects upon the output. Factors laying inside this wedge that present small μ but high σ are deemed to be influential presenting non-linear or interactive effects upon the output (the factor carries the effect of different signs, depending on the values assumed by the other factors). Factors laying inside/outside this wedge that present small μ and σ are deemed to be less/non-influential factors with negligible effects upon the output (Morris, 1991).

2.6. Dynamic calibration of the model being evaluated

The dynamic calibration (based on optimisation algorithms) of the influential input factors of the model consisted of adjusting the simulated TMP (TMP_{SIM}) to the experimental TMP (TMP_{EXP}) by means of the least squares method together with the subspace trust region method (Coleman and Li, 1996), based on the interior-reflective Newton method (implemented in MATLAB® LSQNONLIN), and the Runge-Kutta method (MATLAB® ode45 function). The objective function (*OF*) applied is shown in Eq. 9.

$$OF=\sum\sqrt{\left(TMP_{SIM}-TMP_{EXP}\right)^2} \quad \text{(Eq. 9)}$$

To enhance the dynamic calibration, appropriate initial values for the model factors had to be selected. In this respect, on the basis of the different Morris simulations carried out to select r_{opt}, the optimum initial values chosen were those which combined to give the minimum least squares error between TMP_{SIM} and TMP_{EXP} (see Eq. 9).

Model performance statistical analysis based on the use of the regression line method was performed by using IBM® SPSS® Statistics v.19 and statgraphics® Centurion v.16.2 were used for model performance statistical analysis.

3. Results and discussion

3.1. Sensitivity analysis results

The revised version of the Morris screening method was applied to different number of trajectories (r), chosen from M =1000 initial Morris trajectories, until the ranking of significant factors remained more or less stable, as measured quantitatively by the index $PF_{ri \rightarrow rj}$. Factor uncertainty was set to 20% of the variability of the default values shown in Table 2. This value was established on the basis of the results from different trials in which uncertainty ranged from 10 to 50%.

Table 3 shows the resulting μ^* from the model inputs calculated for the different number of runs selected for the Morris simulations. As Table 3 illustrates, higher numbers of runs (i.e. an increase in r) did not significantly modify the sensitivity measures of the inputs. For instance, increasing the number of runs from 10 to 40 had no significant impact on the rankings of the different model factors.

Table 4 shows $PF_{ri \rightarrow rj}$ for the different number of trajectories evaluated. As can be seen in Table 4, $PF_{ri \rightarrow rj}$ was low even when the number of runs was low (e.g. r = 10~40). This means that in this study, values of r below 40 (e.g. r = 10~30) give a suitable estimate of sensitivity measurements. These results tally with other applications of the Morris screening method involving few repetitions (e.g. r = 10~20) (Campolongo et al., 2011; Ruano et al., 2011).

As previously commented, achieving two consecutives $PF_{ri \rightarrow rj}$ values below 0.3 (i.e. $PF_{ri \rightarrow rj}$ values below 30% of PF_{MAX}) was established as the criteria for establishing r_j as r_{opt}. In this respect, $PF_{ri \rightarrow rj}$ resulted in a value of 0.3 when r was increased (from 10 to 20) and remained below this threshold value at higher r (from 20 to 40). On the basis of these results, r = 20 was selected as the optimal number of repetitions (r_{opt}) in this study. r = 20 was considered to be optimal not only because $PF_{10 \rightarrow 20}$ was low but also

because of the significant stability of the factors at the top of the ranking (see Table 3). In addition, similar results regarding the significant stability of the factors at the ranking were obtained for the case of r = 10~40, since $PF_{ri \rightarrow rj}$ remained close to zero. When r_{opt} = 20, 300 simulations (simulations = $r \cdot (k+1)$; r = 20; k = 14) were required to evaluate the entire model. One simulation (covering 1 month's operations) took approximately 10 minutes to calculate using a PC with 8 GHz Intel® CORE™ i5 processor. Therefore, in this study, it was possible to estimate the sensitivity measures adequately with a low number of repetitions (requiring few calculations). These results suggest adequate coverage of the input space and, therefore, that possible problems related to type I error (i.e. considering a factor to be significant when it is not) and type II error (i.e. failing to identify a factor that influences the model considerably) are minimised.

Figure 1 shows the graphical Morris approach for the optimal number of repetitions selected for the sensitivity evaluation. This figure shows the most influential input factors in the model. Figure 1a shows the 6 most influential input factors, which lie outside the wedge formed by two lines plotted according to $\mu_i = \pm 2SEM_i$. They have means substantially different from 0 and relatively small standard deviations. It consisted of: (1) the model factor related to reversible fouling γ_0 (μ = -0.527 and σ = 0.185); (2) the model factor related to reversible fouling β_2 (μ = -0.159 and σ = 0.090); (3) the model factor related to reversible fouling β_1 (μ = -0.112 and σ = 0.068); (4) the factor related to sub-critical fouling k_{SF} (μ = -0.089 and σ = 0.051); (5) the fouling rate when J_{20} tends to zero K_F (μ = -0.060 and σ = 0.038); and (6) the maximum membrane scouring velocity $q_{MS,Max}$ (μ = 0.051 and σ = 0.034). It is important to note that 3 of the 4 model factors in the sigmoid inhibition function (see Eq. 5) included in process 2 (cake layer removal using biogas sparging to scour the membrane) had the highest mean

and standard deviation values: γ_0, β_2 and β_1. These results highlight the importance of these factors for an adequate representation of the filtration results achieved using the developed model. It is important to note that the calibration method proposed for these factors (in addition to K_F) entailed off-line experiments based on the data obtained from different flux-step trials according to Robles et al. (2012). The next in importance were k_{SF}, $q_{MS,Max}$ and K_F. These 3 factors are also related to the reversible fouling mechanisms modelled.

In particular, it is important to highlight the great influence of the factor γ_0, which has the highest μ (in absolute term) and σ. According to the Morris theory, factors with high σ are expected to have a non-linear or interactive impact on output. Indeed, based on the defined model, γ_0 modifies the impact of other inputs on the model output (interactions between input factors). Finally, γ_0 determines the critical filtration conditions for given MLTS and BRF, and thus affects the final value of ω_C at given operating conditions. Therefore, γ_0 indirectly determines the final value of ω_I, which is a direct function of ω_C and $q_{IF,Max}$. Both ω_C and ω_I finally determine the model output (TMP). Behaviour similar to γ_0 but to a lesser extent was observed for β_2 and β_1 (both affect critical filtration conditions). On the other hand, the impacts of k_{SF}, $q_{MS,Max}$ and K_F upon output are expected to be more linear and additive: their mean is quite high and their standard deviation not very high. This behaviour is desirable when estimating factors on the basis of optimisation algorithms.

Six model factors were identified as less/non-influential input factors (see Figure 1b): (1) specific resistance of cake at zero pressure $\alpha_{C,0}$ (μ = -0.018 and σ = 0.004); (2) proportional constant k_{RI} (μ = -0.009 and σ = 0.009); (3) maximum irreversible fouling

kinetic constant $q_{IF,Max}$ (μ = -0.006 and σ = 0.009); (4) half-saturation coefficient for cake solids during membrane scouring and back-flushing $K_{S,X_{m_C}}$ (μ = -0.005 and σ = 0.003); (5) average specific irreversible fouling resistance α_I (μ = -0.004 and σ = 0.006); and (6) pressure needed to double specific resistance TMP_a (μ = 0.010 and σ = 0.004). It is important to highlight that 3 of the 7 factors identified as less/non-influential are related to irreversible fouling: $q_{IF,Max}$, α_I and k_{RI}. The low impact of these factors on the model output was attributed to the expected non-linear or interactive impact on the output of the influential input factors related to reversible fouling.

One aspect to highlight is that only two model factors, the time constant k_t and the maximum back-flushing removal velocity $q_{BF,Max}$, were identified as non-influential with a value of zero for both sensitivity measures (μ and σ). The value of k_t is related to the time required for compressing the cake to its equilibrium value for a given TMP level (i.e. increasing α_C to $\alpha_{C,TMP}$). In this respect, it was assumed that $\alpha_{C,TMP}$ was always achieved independently of the value established for k_t within the selected input uncertainty. The effect of this input factor (k_t) on the output is therefore expected to be negligible, therefore this result suggests it is not necessary to calibrate this input factor in this particular application of the model. On the other hand, $q_{BF,Max}$ gives the maximum back-flushing removal velocity. Since this factor was identified as non-influential, it can be assumed that for the back-flushing duration interval evaluated in this study (from 30 to 50 seconds), the reversible cake-layer was completely removed from the membrane surface. Moreover, it is interesting to note that low back-flushing frequencies (1 back-flushing for each 10 filtration-relaxation cycles on average) were applied, therefore this input factor was expected to influence the output less than other inputs (e.g. the input factors related to the removal of fouling by using biogas sparging

to scour the membrane).

Input factors identified as less/non-influential can be set to default values based on optimisation algorithms. It must be emphasised that these factors are for the input factors whose values were not calibrated off-line beforehand. To be precise, these factors were either dynamically calibrated ($\alpha_{C,0}$ and TMP_a), or calculated on the basis of experimental data ($q_{IF,Max}$, $K_{S,X_{m_C}}$ and k_{RI}), or set to default values (α_I, $q_{BF,Max}$ and k_t).

3.2. Assessment of the modelling approach

As mentioned before, one main characteristic of the model evaluated in this study is that it was developed on the basis of the operating results of an AnMBR system fitted with industrial-scale membranes. Hence, most of the factors included in the model were defined in order to represent all possible filtration process performances. Indeed, the results of the sensitivity analysis tally with the knowledge of the process because most of the proposed model factors defined and calibrated by off-line experiments were identified as the most influential input factors. In this respect, the factors related to membrane scouring (β_1, β_2, γ_0, K_F and $q_{MS,Max}$) were defined in the model on the basis of trials designed to identify the critical filtration conditions of the AnMBR plant.

As regards the less/non-influential input factors, those related to cake layer build-up and compression during filtration (k_{SF}, $\alpha_{C,0}$ and TMP_a) and cake layer removal during back-flushing ($K_{S,X_{m_C}}$) were included in the model on the basis of experimental results found in recent literature (Bugge et al., 2012; Jørgensen et al., 2012; Sarioglu et al., 2012). As regards irreversible fouling mechanisms, factors $q_{IF,Max}$, α_I and k_{RI} were

included in the model on the basis of experimental results concerning long-term membrane performance (i.e. on the basis of the results showing an increase in the total filtering resistance of the system and a decrease in the critical flux determined in experiments throughout the operating period of the plant).

As regards the input factors identified in this study as non-influential (k_t and $q_{BF,Max}$), the result obtained for k_t predicts that this factor can be fixed to a constant value in the model. The result for $q_{BF,Max}$ suggests that this input factor is not required in the model definition although this factor was identified as non-influential in this specific study in which low back-flushing frequencies were applied. Therefore, it must be said that this input factor is expected to model the output in other specific situations or model applications (e.g. operating with variable duration, high back-flushing frequencies, modelling short-term process performance, etc.).

3.3. Model calibration

For the experimental period evaluated in this study, the 6 influential input factors (β_1, β_2, γ_0, K_F, $q_{MS,Max}$, k_{SF}) were calibrated by an optimisation algorithm, and the other factors were set to the optimised initial values. Table 5 shows the initial values used in this dynamic calibration (column 1) and the calibrated values for the influential input factors mentioned above (column 2). It is important to highlight the results obtained from the dynamic calibration of the highly-influential factors that were previously calibrated by off-line experiments (i.e. β_1, β_2, γ_0, K_F and $q_{MS,Max}$). Specifically, similar values were obtained for these influential factors when calibrated either dynamically or experimentally (see Table 2 and Table 5). Hence, suitable estimation of these factors can be obtained when using parameter estimation methods.

Figure 2 shows the results of the dynamic model calibration. Figure 2a shows the average daily values of J_{20net}, BRF, and MLTS. Figure 2b shows the average daily TMP_{SIM} and TMP_{EXP}. Hence, Figure 2 shows that, even when operating at different MLTS, J_{20net} and BRF levels (see Figure 2a), the model accurately predicted the membrane performance using the calibrated values for the model factors (see Figure 2b): an adequate Pearson Product-Moment correlation coefficient (R) between TMP_{EXP} and TMP_{SIM} was obtained (0.947). Nevertheless, the model also gave accurate results when using the default values (Pearson's R coefficient was 0.898). Hence, the performance of the model was only slightly enhanced by dynamically calibrating the influential model factors because the initial factor values had been calibrated previously using long-term data (Robles et al., 2013a).

In order to validate the results obtained using the dynamically calibrated filtration model, the regression line method was used in this study.

Figure 3a shows the scatter plot of the pairs of modelled and observed TMP data values of the dynamically calibrated filtration model for the same point in time, i.e. the modelled output values are plotted against the corresponding measured (observed) data. According to the results shown in Figure 3a, the relationship between modelled and observed data can be visually described as linear model. Specifically, this linear model significantly approximates to an ideal, unbiased model since it yields a slope line similar to a unity-slope line through the origin (slope and intercept approximate to 1 and 0, respectively). In addition, no systematic divergence from the slope line is observed, which indicates non unmodelled behaviour (i.e. underestimation or overestimation). In this respect, the R-Squared statistic indicates that the model as fitted explains 89.72% of

the variability in the modelled TMP.

The resulting P-value in the Analysis of Variance (ANOVA) of the results shown in Figure 3a resulted in a value lower than 0.05 (P-value = 0.0000). Therefore, there is a statistically significant relationship between the modelled and observed TMP at the 95.0% confidence level. Moreover, a hypothesis contrast was conducted to evaluate whether the linear regression model slope is significantly different from the unit. This hypothesis contrast resulted in a P-value above 0.05, validating the null hypothesis for which the slope equals the unit. Therefore, it can be drawn that there are no statistically significant differences between the modelled and observed TMP at the 95.0% confidence level. In addition, as mentioned before, the corresponding Pearson Product-Moment correlation coefficient (R) between modelled and observed values equals 0.947, indicating a relatively strong relationship between the variables.

Figure 3b shows the studentised residuals, which are the quotient resulting from the division of a residual (the difference between observed and modelled data) by an estimate of its standard deviation (Student's t-statistic), resulting from the linear regression model shown in Figure 3a. Specifically, Figure 3b shows the studentised residual error as dependent variable and the simulation time as descriptor variable. This plot does not reveal high unmodelled behaviour since a nearby uniform spread of residuals is observed (i.e. there is systematic difference from cero and not systematic changes over the descriptor variable). Nevertheless, a slightly higher density of positive values can be observed in this figure, indicating that the dynamically calibrated model slightly tends to overestimate correct values. As Figure 3b shows, two observations resulted in studentised residuals greater than 2 in absolute value, but no observations resulted in values higher than 3 in absolute terms. Therefore, outliers were not

identified.

On the other hand, the Durbin-Watson (DW) statistic was calculated, which tests the residuals in order to determine if there is any significant correlation. According to Figure 3b, DW indicated a possible serial correlation at the 95.0% confidence level since the P-value is less than 0.05 (DW = 1.190). The plot of standardised residuals vs. standardised modelled values resulted in a uniform scatter of the pairs of values, which indicated that the variance is statistically uniform (i.e. homocedasticity of the predictive model). Finally, Kolmogorov-Smirnov-Lilliefors test was performed to assess normality in the residuals. This test resulted in a P-value > 0.05, thus the stochastic character of the error was statistically confirmed.

Therefore, the statistical analysis confirmed the validity of the results obtained from the dynamically calibrated filtration model.

4. Conclusions

A sensitivity analysis of a filtration model for AnMBRs using a revised version of the Morris screening method was conducted. The optimal number of repetitions found in this study (r_{opt} = 20) was similar to the number of repetitions mainly used in other applications of the Morris screening method. Using the Morris screening method enabled to validate the model: 6 of the model's 14 factors were identified as influential, i.e. the factors calibrated using off-line methods. This tallied with the knowledge of the process because the model was developed on the basis of experimental results.

Acknowledgements

This research work has been supported by the Spanish Ministry of Economy and Competitiveness (MINECO, Projects CTM2011-28595-C02-01/02) jointly with the European Regional Development Fund (ERDF) which are gratefully acknowledged.

References

[1] American Public Health Association/American Water Works Association/Water Environmental Federation, 2005. Standard methods for the Examination of Water and Wastewater, 21st edition, Washington DC, USA.

[2] Bugge, T.V., Jørgensen, M.K., Christensen, M.L., Keiding, K., 2012. Modeling cake buildup under TMP-step filtration in a membrane bioreactor: Cake compressibility is significant. Water Res. 46, 4330 – 4338.

[3] Campolongo, F., Cariboni, J., Saltelli, A., 2007. An effective screening design for sensitivity analysis of large models. Environ. Mod. Soft. 22, 1509 – 1518.

[4] Campolongo, F., Saltelli, A., Cariboni, J., 2011. From screening to quantitative sensitivity analysis. A unified approach. Comput. Phys. Commun. 182, 978 – 988.

[5] Coleman, T.F., Li, Y., 1996. An interior, trust region approach for nonlinear minimization subject to bounds. SIAM J. Optim. 6, 418 – 445.

[6] Copp, J.B., 1999. Development of standardised influent files for the evaluation of activated sludge control strategies, IAWQ Scientific and Technical Report Task Group: Respirometry in Control of the Activated Sludge Process – internal report.

[7] A. Cosenza, G. Mannina, P.A. Vanrolleghem, M.B. Neumann, Global sensitivity analysis in wastewater applications: a comprehensive comparison of different methods. Environ. Mod. Soft. 49 (2013), 40 – 52.

[8] Cropp, R., Braddock, R., 2002. The New Morris method: an efficient second-order screening method. Reliab. Eng. Syst. Safe., 78, 77 – 83.

[9] Derbal, K., Bencheikh-lehocine, M., Cecchi, F., Meniai, A.-H., Pavan, P., 2009. Application of the IWA ADM1 model to simulate anaerobic co-digestion of organic waste with waste activated sludge in

mesophilic condition. Bioresour. Technol. 100, 1539 – 1543.

[10] Drews, A., 2010. Membrane fouling in membrane bioreactors – Characterisation, contradictions, cause and cures. J. Membr. Sci. 363, 1 – 28.

[11] Ferrer, J., Morenilla, J.J., Bouzas, A., García-Usach, F., 2004. Calibration and simulation of two large wastewater treatment plants operated for nutrient removal. Water Sci. Technol. 50, 87 – 94.

[12] Jørgensen, M.K., Bugge, T.V., Christensen, M.L., Keiding, K., 2012. Modeling approach to determine cake buildup and compression in a high-shear membrane bioreactor. J. Membrane Sci. 409/410, 335 – 345.

[13] Mannina, G., Di Bella, G., Viviani, G., 2011. An integrated model for biological and physical process simulation in membrane bioreactors (MBRs). J. Membrane Sci. 376, 56 – 69.

[14] Morris, M., 1991. Factorial sampling plans for preliminary computational experiments. Technometrics. 33, 239 – 245.

[15] Naessens, W., Maere, T., Nopens, I., 2012. Critical review of membrane bioreactor models – Part 1: Biokinetic and filtration models Bioresour. Technol. 122, 95 – 106.

[16] Ng, A.N.L., Kim, A.S., 2007. A mini-review of modeling studies on membrane bioreactor (MBR) treatment for municipal wastewaters. Desalination 212, 261 – 281.

[17] Robles, A., Ruano, M.V., García-Usach, F., Ferrer, J., 2012. Sub-critical filtration conditions of commercial hollow-fibre membranes in a submerged anaerobic MBR (HF-SAnMBR) system: The effect of gas sparging intensity. Bioresour. Technol. 114, 247–254.

[18] Robles, A., Ruano, M.V., Ribes, J., Seco, A., Ferrer, J., 2013a. A filtration model applied to submerged anaerobic MBRs (SAnMBRs). J. Membrane Sci. 444, 139 – 147.

[19] Robles, A., Ruano, M.V., Ribes, J., Seco, A., Ferrer, J., 2013b. Mathematical modelling of filtration in submerged anaerobic MBRs (SAnMBRs): long-term validation. J. Membrane Sci. 446, 303 – 309.

[20] Robles, A., Ruano, M.V., Ribes, J., Ferrer, J., 2013c. Factors that affect the permeability of commercial hollow-fibre membranes in a submerged anaerobic MBR (HF-SAnMBR) system. Water Res. 47, 1277 – 1288.

[21] Robles, A., Ruano, M.V., Ribes, J., Ferrer, J., 2013d. Advanced control system for optimal filtration in submerged anaerobic MBRs (SAnMBRs). J. Membrane Sci. 430, 330 – 341.

[22] Ruano, M.V., Ribes, J., Ferrer, J., Sin, G., 2011. Application of the Morris method for screening the influential parameters of fuzzy controllers applied to WWTPs. Wat. Scien. Tech. 63, 2199 – 2206.

[23] Ruano, M.V., Ribes, J., Seco, A., Ferrer, J., 2012a. An improved sampling strategy based on trajectory design for the application of Morris method to systems with many input factors. Environ. Mod. Soft. 37, 103 – 109.

[24] Ruano, M.V., Serralta, J., Ribes, J., Garcia-Usach, F., Bouzas, A., Barat, R., Seco, A., Ferrer, J., 2012b. Application of the General Model "Biological Nutrient Removal Model No.1" to upgrade two full-scale WWTPs. Environ. Technol. 33, 1005 – 1012.

[25] Saltelli, A., Tarantola, S., Campolongo, F., Ratto, M., 2004. Sensitivity analysis in practice: a guide to assessing scientific models. Chicester: Wiley.

[26] Sarioglu, M., Insel, G., Orhon, D., 2012. Dynamic in-series resistance modeling and analysis of a submerged membrane bioreactor using a novel filtration mode. Desalination 285, 285 – 294.

[27] Sin, G., Gernaey, KV., 2009. Improving the Morris method for sensitivity analysis by scaling the elementary effects, In: proceedings of the 19th European Symposium on Computer Aided Process Engineering (ESCAPE 19), 925 – 930.

Figure and table captions

Table 1. Stoichiometry and kinetic expressions of the processes considered in the model.

Table 2. Default values of factors in the evaluated filtration model. Uncertainty was set to 20% of the variability of these values in the dynamics simulations.

Table 3. Sensitivity analysis results: sensitivity measures of the model factors for the different values of *r* evaluated (r_{opt} = 20).

Table 4. Sensitivity analysis results: position factors ($PF_{ri \rightarrow rj}$) for the *r* evaluated.

Table 5. Initial and dynamically calibrated values for the different model factors in the experimental period evaluated in this study.

Figure 1. (a) Sensitivity analysis results: μ versus σ for the final value of r_{opt} of 20. **(b)** Zoom of the sensitivity analysis results in the range of - 0.025 < μ < 0.025 and 0 < σ < 0.02. Lines correspond to $\mu_i = \pm 2\ SEM_i$.

Figure 2. Model validation using the optimised model factors values. Average daily values of **(a)** MLTS, J_{20net} and BRF and **(b)** TMP_{EXP} and TMP_{SIM}. * *R represents the Pearson Product-Moment correlation coefficient between* TMP_{EXP} *and* TMP_{SIM}.

Figure 3. (a) Scatter plot of the pairs of modelled and observed TMP data of the dynamically calibrated filtration model for the same point in time. **(b)** Studentised residuals resulting from the linear model representing the relationship between modelled and observed TMP data

Table 1. Stoichiometry and kinetic expressions of the processes considered in the model.

Component i / Process j	X_{TS}	X_{m_C}	X_{m_I}	*Kinetic expression*
1. Cake layer formation	-1	1		$Q_{20P} \cdot X_{TS}$
2. Membrane scouring by biogas	1	-1		$q_{MS,Max} \cdot M_{X_{m_C}} \cdot I_{MS} \cdot BRF_V \cdot X_{m_C}$
3. Cake layer detachment during back-flushing	1	-1		$q_{BF,Max} \cdot Q_{20BF} \cdot M_{X_{m_C}} \cdot X_{m_C}$
4. Irreversible fouling consolidation		-1	1	$q_{IF,Max} \cdot X_{m_C}$

Table 2. Default values of factor in the evaluated filtration model. Uncertainty was set to 20% of the variability of these values in the dynamics simulations.

Factor	Units	Default value
$q_{MS,Max}$		6.31
$q_{BF,Max}$	m^{-3}	1
$q_{IF,Max}$	s^{-1}	$3 \cdot 10^{-07}$
$K_{S,XmC}$	kg SST	0.2
$\alpha_{C,0}$	m kg^{-1}	$1.02 \cdot 10^{13}$
TMP_a	kPa	18.9
k_t	s^{-1}	1
k_{SF}	m kg^{-1} s^{-1}	$4.09 \cdot 10^{10}$
K_F	Pa s^{-1}	$5.6 \cdot 10^{-4}$
β_1	s^2 m^{-1}	$-2.48 \cdot 10^{8}$
β_2	s m^2 kg^{-1}	$5.1 \cdot 10^{4}$
γ_0	s m^{-1}	$2.81 \cdot 10^{6}$
k_{RI}	s	$1.6 \cdot 10^{-07}$
α_I	m kg^{-1}	$1 \cdot 10^{14}$

Table 3. Sensitivity analysis results: sensitivity measures of the model factors for the different values of *r* evaluated (r_{opt} = 20).

r = 10		***r = 20***	
Factor	***μ****	**Factor**	***μ****
γ_0	0.496	γ_0	0.547
β_2	0.151	β_2	0.159
k_{SF}	0.096	β_1	0.119
β_1	0.092	k_{SF}	0.089
K_F	0.046	$q_{MS,Max}$	0.060
$q_{MS,Max}$	0.046	K_F	0.051
$\alpha_{C,0}$	0.016	$\alpha_{C,0}$	0.018
k_{RI}	0.010	k_{RI}	0.010
TMP_a	0.009	TMP_a	0.009
$K_{S,XmC}$	0.004	$K_{S,XmC}$	0.007
$q_{IF,Max}$	0.004	$q_{IF,Max}$	0.005
α_I	0.003	α_I	0.004
k_t	0.000	k_t	0.000
$q_{BF,Max}$	0.000	$q_{BF,Max}$	0.000

r = 30		***r = 40***	
Factor	***μ****	**Factor**	***μ****
γ_0	0.599	γ_0	0.527
β_2	0.182	β_2	0.159
β_1	0.128	β_1	0.116
k_{SF}	0.097	k_{SF}	0.090
K_F	0.068	$q_{MS,Max}$	0.054
$q_{MS,Max}$	0.062	K_F	0.051
$\alpha_{C,0}$	0.015	$\alpha_{C,0}$	0.015
TMP_a	0.015	k_{RI}	0.010
k_{RI}	0.008	TMP_a	0.008
$q_{IF,Max}$	0.006	$K_{S,XmC}$	0.005
$K_{S,XmC}$	0.005	$q_{IF,Max}$	0.003
α_I	0.005	α_I	0.003
k_t	0.000	k_t	0.000
$q_{BF,Max}$	0.000	$q_{BF,Max}$	0.000

Table 4. Sensitivity analysis results: position factors ($PF_{ri \to rj}$) for the *r* evaluated.

$r_i \to r_j$	$10 \to 20$	$20 \to 30$	$30 \to 40$
$PF_{ri \to rj}$	0.07	0.06	0.06

Table 5. Initial and dynamically calibrated values for the different model factors in the experimental period evaluated in this study.

Factor	Unit	Initial value	Calibrated value
$q_{MS,Max}$		5.89	4.71
$q_{BF,Max}$	m^{-3}	1.07	
$q_{IF,Max}$	s^{-1}	$3 \cdot 60^{-07}$	
$K_{S,XmC}$	kg SST	0.19	
$\alpha_{C,0}$	m kg^{-1}	$1.08 \cdot 10^{13}$	
TMP_a	kPa	20.1	
k_t	s^{-1}	1.2	
k_{SF}	m kg^{-1} s^{-1}	$3.81 \cdot 10^{10}$	$2.30 \cdot 10^{10}$
K_F	Pa s^{-1}	$4.5 \cdot 10^{-4}$	$5.4 \cdot 10^{-4}$
β_1	s^2 m^{-1}	$-2.31 \cdot 10^{8}$	$-1.85 \cdot 10^{8}$
β_2	s m^2 kg^{-1}	$4.1 \cdot 10^{4}$	$4.9 \cdot 10^{4}$
γ_0	s m^{-1}	$2.62 \cdot 10^{6}$	$3.14 \cdot 10^{6}$
k_{RI}	s	$1.9 \cdot 10^{-07}$	
α_I	m kg^{-1}	$1 \cdot 20^{14}$	

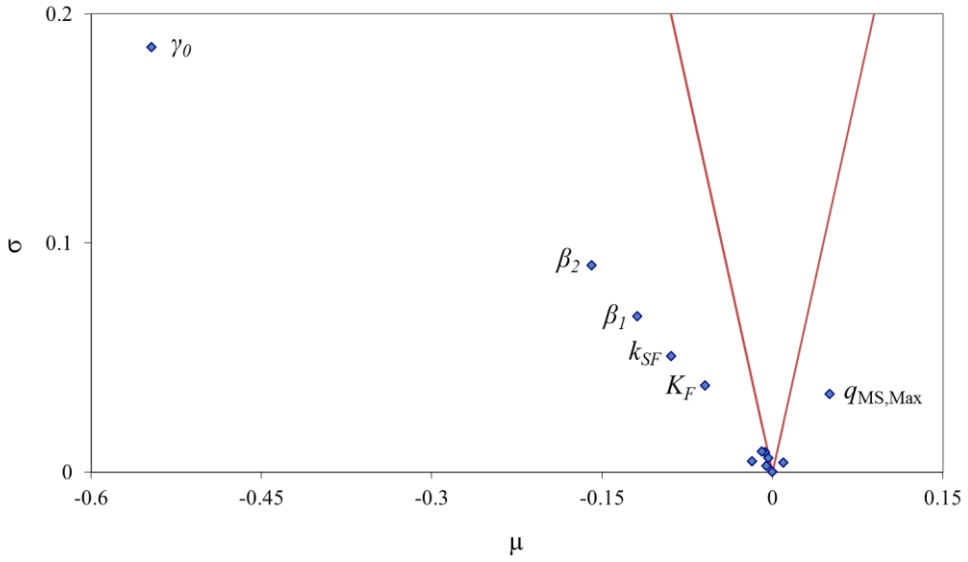

(a)

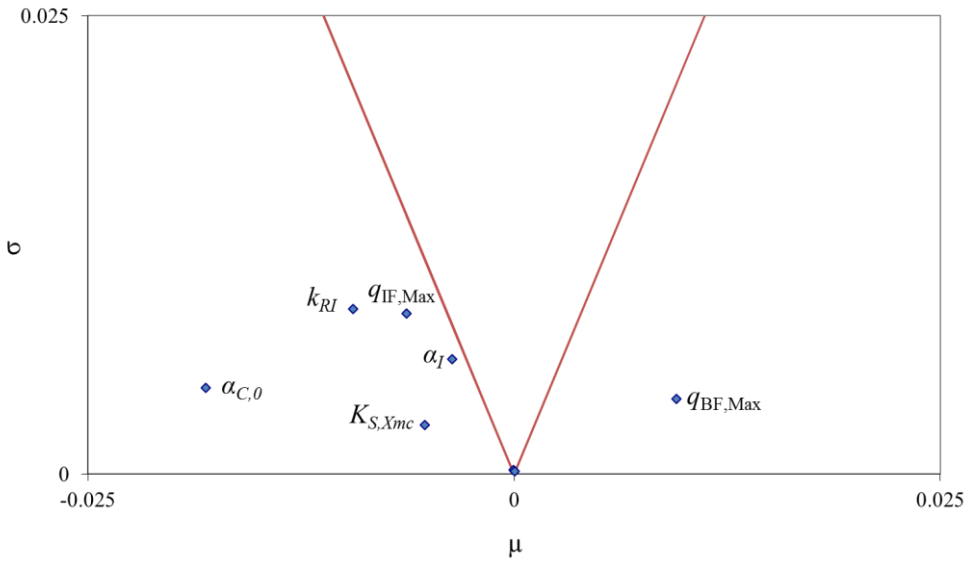

(b)

Figure 1. (a) Sensitivity analysis results: μ versus σ for the final value of r_{opt} of 20. **(b)** Zoom of the sensitivity analysis results in the range of - 0.025 < μ < 0.025 and 0 < σ < 0.02. Lines correspond to $\mu_i = \pm 2\ SEM_i$.

.

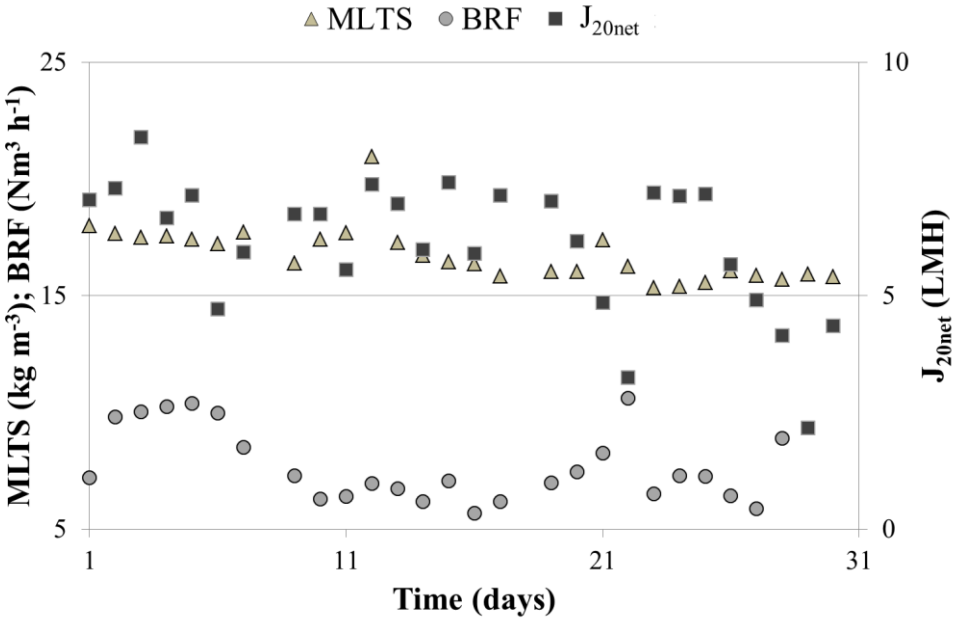

(a)

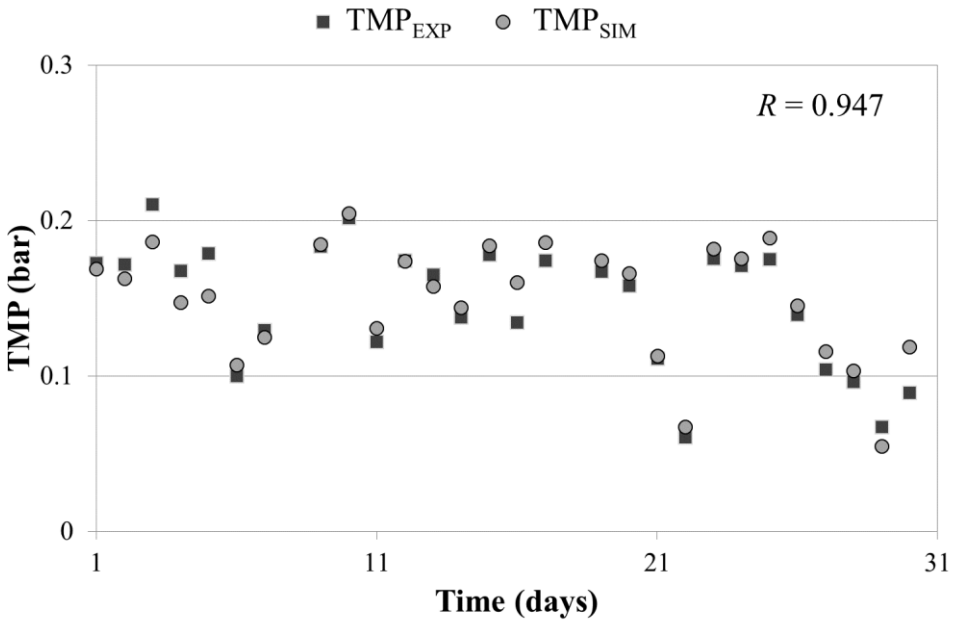

(b)

Figure 2. Model validation using the optimised model factor values. Average daily values of **(a)** MLTS, J_{20net} and BRF and **(b)** TMP_{EXP} and TMP_{SIM}. * *R represents the Pearson Product-Moment correlation coefficient between TMP_{EXP} and TMP_{SIM}.*

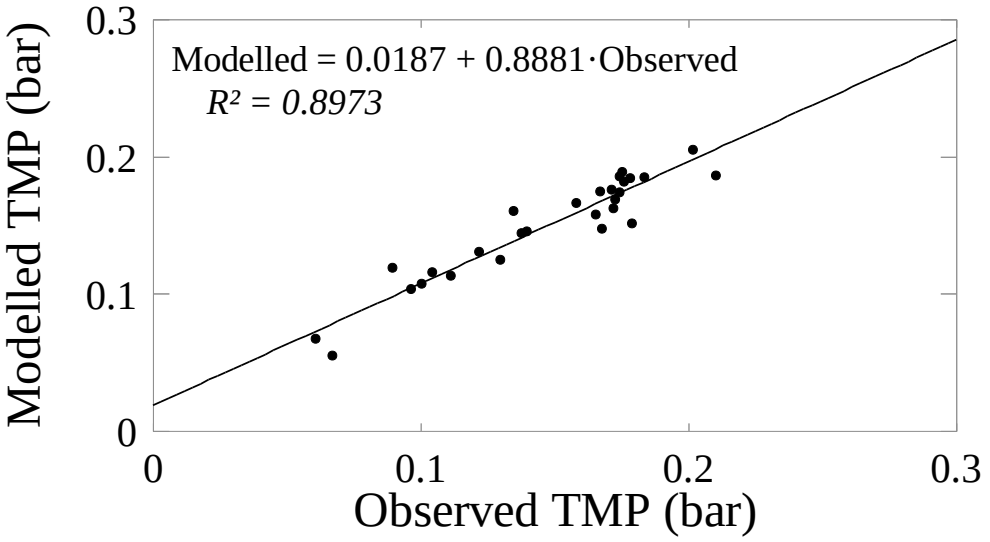

(a)

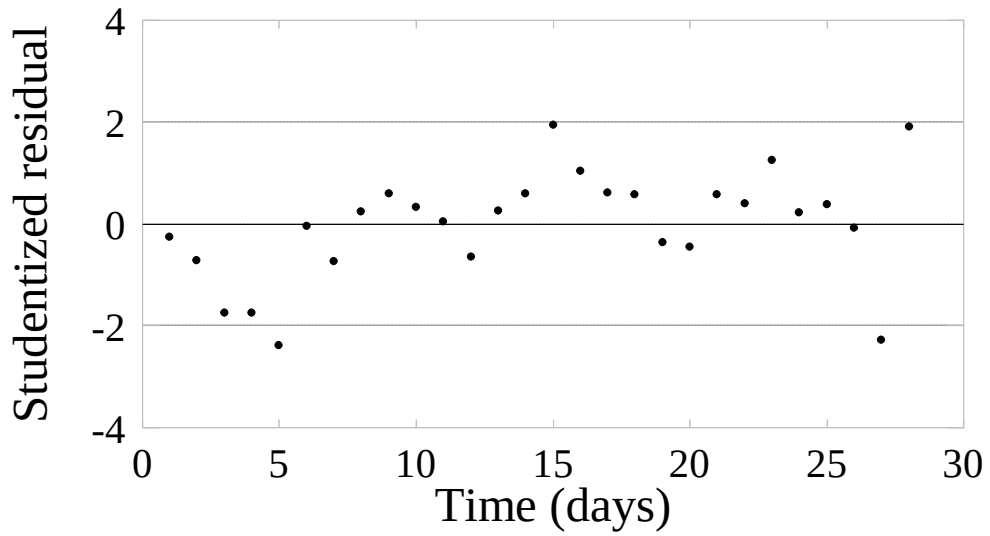

(b)

Figure 3. (a) Scatter plot of the pairs of modelled and observed TMP data of the dynamically calibrated filtration model for the same point in time. **(b)** Studentised residuals resulting from the linear model representing the relationship between modelled and observed TMP data.